SINTEF REPORT

SINTEF ICT

Address:
NO-7031 Trondheim
NORWAY
Location:
S P Andersens v 15
NO-7031 Trondheim
Telephone: +47 73 59 30 00
Fax: +47 73 59 29 30

Enterprise No.: NO 948 007 029 MVA

TITLE

Mathematical modelling of seismic noise- model description and documentation

AUTHOR(S)

Jens M. Hovem

CLIENT(S)

Norwegian Petroleum Directorate (NPD)

REPORT NO.	CLASSIFICATION	CLIENTS REF.	
SINTEF A14560	Open	Jan Stenløkk	
CLASS. THIS PAGE	ISBN	PROJECT NO.	NO. OF PAGES/APPENDICES
Open	978-82-14-04466-9	90E322	22
ELECTRONIC FILE CODE		PROJECT MANAGER (NAME, SIGN.)	CHECKED BY (NAME, SIGN.)
Report 1 Documentation of the basemodel.doc		Jens M. Hovem	Odd Kr. Ø. Pettersen
FILE CODE	DATE2	APPROVED BY (NAME, POSITION, SIGN.)	
	2010-01-25	Odd Kr. Ø. Pettersen, Research Director	

ABSTRACT

The objective of this project is to use a mathematical model for the propagation of seismic airgun signals in the water column and to forecast the effect such signals and noise may have on fish and animals in the sea. The model used is the PlaneRay model, a model based on ray theory that can deal with range-dependent bathymetry and depth-dependent sound speed variations. The seismo-acoustic properties of a layered seabed with absorption and shear wave conversion are included in an approximated manner. The model can simulate the total sound field, both in the time and in the frequency domain, out to very large distances. In cases where the ray modelling may be suspect because of its inherent limitations other codes based on different mathematical approaches may supplement the ray model. In this report the wave number integration model called OASES model is used for quality control and benchmarking. The report contains several examples of modelling of synthetic, but relevant scenarios. The result of PlaneRay and OASES are compared and discussed with the objective to understand the limitations of validity potential errors of the codes. A short users guide to the PlaneRay code is included in the appendix.

KEYWORDS	ENGLISH	NORWEGIAN
GROUP 1	Acoustics	Akustikk
GROUP 2	Modeling	Modellering
SELECTED BY AUTHOR	Seismic noise	Seismisk støy
	Propagation	Propagasjon

TABLE OF CONTENTS

1 Background and introduction

The fishing industry and the oil and gas companies has conflicting views on the impact on fishing resulting from the coustic and seismic noise associated with marine seismic exploration. The fishing industry states that air gun noise affects the behaviour and scares fish away from the fishing grounds thus resulting in reduced catches. This is disputed by the seismic companies claiming the noise level and the scaring effect is greatly exaggerated. This conflict of interest has motivated the Norwegian Petroleum Directorate (NPD) to commission SINTEF ICT and Department of Biology at the University of Oslo with the task of developing a capability of predicting the sound level and other characteristics of the acoustic noise field of air guns arrays, and to combine this with new knowledge of how the various fish species hear and react to the noise.

Marine seismic exploration uses airguns or airgun arrays to generate high energy, short duration acoustic pulses into the subsea strata. These pulses are reflected back to receivers (hydrophones) in the water. By studying the structure of the received signal, the geophysicists draw conclusions about the structure of the underground. The airguns and airgun arrays are configured to maximize the downward transmission into the bottom; approximately 90 % of the acoustic energy is converted to seismic energy in the seafloor. However, some of the energy is transmitted to the water and reflected at the bottom and sea surface and therefore remains in the water column: This acoustic energy is quite significant because the energy level of the source is quite high and the noise signals can propagate to considerably distances and may cause disturbance to marine life, such as fish and sea animals.

This report is only on models for the propagation of air gun noise, firsts by discussing the advantages and disadvantages of the various theoretical approaches and then presenting the model of choice. This model, PlaneRay, is based on ray tracing and can deal with range-dependent bathymetry and depth-dependent sound speed variations. The seismo-acoustic properties of a layered seabed with absorption and shear wave conversion are included in an approximated manner. The model can simulate the total sound field, both in the time and in the frequency domain, out to very large distances. In cases where the ray modelling may be suspect because of its inherent limitations the OASES model will be used for quality control and benchmarking. This report therefore contains several examples where the two approaches are compared.

The problem of modelling this transient noise field is in many aspects different from the normal seismic modelling problem since we now are not interested in the wave field in the underground, but only the wave field in the water column. This difference on focus requires a different approach than the seismic modelling.

The frequency range of interest is approximately from 25 - 50 Hz, and up to 1000 Hz. At these frequencies the geoacoustic properties of the seabed are important for the conversion of acoustic energy in the water to acoustic/seismic energy in the bottom important. Furthermore, range dependent model capability is required because the actual scenarios may have a water depth and environmental properties that dependent on the locations. In many ways the problem is similar to the problem encountered in passive sonar for surveillance of submarines and ships based on their emitted acoustic noise. The frequency range is approximately the same, but in the seismic noise problem we are dealing with transient signals and not steady state signals as in passive sonar. This requires that the model can predict the full wave form and time structure of the signals and not only the sound level.

Modelling of acoustic propagation conditions has always been an important issue in underwater acoustics and there exist several mathematical/numerical models based on different methods (Jensen et al. (1993)]. The most common models are based on normal modes [Jensen and Ferla (1979), Clark and Smith (2008)], the parabolic equation [Collins (1993), Colis et al. (2008)], models based on the wave number integration technique [Schmidt (1987, 2004), Goh and Schmidt (1996)] and the ray tracing models [Jensen et al.(1993), Westwood and Vidmar (1987), Westwood and Tindle(1987)]. Some of these models can deal range dependent problems. Ray tracing models, the oldest and simplest type of models, have for some time been considered outdated as compared with the more sophisticated models mentioned above. However, in recent years there seems to be a renewed interest for ray tracing models, also for long range, low frequency applications [Hovem (2008]. Ray tracing models are computationally quite efficient since the main calculation of ray trajectories is independent of frequency; the frequency enters only through the interaction with the boundaries, sea surface and sea floor, and can be introduced separately.

In a preliminary study of available models and their capabilities we have come to the conclusion to use principally the ray trace model PlaneRay, but supplemented with the wave number integration model OASES. The ray approach has limited accuracy at very low frequencies (less than 25 Hz in the current application) and the effects of the bottom interaction are treated in an approximate manner. The OASES model is more accurate for these reasons, but has other practical limitations since it is quite difficult to use and can only a handle range independent situations with no variation in water depth and bottom parameters with range. For this reason we will in addition to the PlaneRay model also use the OASES model to verify the results in situations where the application of ray theory may be suspect. The two models are complimentary and therefore both will be used in the analysis and evaluations.

This report features a number of cases where the ray trace result of PlaneRay is compared with the wave number integration technique results with OASES. In general the two set of results agree quite good. The PlaneRay model is therefore considered to have acceptable accuracy for the study of fish reactions to seismic noise, but will be supplemented with OASES in certain limited cases.

2 The PlaneRay model

Figure 1 shows the general propagation problem that can be modeled with the ray model called PlaneRay. The sound speed profile in the water is limited to be a function of only depth and is not allowed to vary in the horizontal direction. The receivers are located on a horizontal line in the water. Rays are only traced to the water-sediment interface and not into the bottom and acoustic effect of the bottom is represented by plane ray reflections coefficients. The bottom may be layered and, in principle, any number of fluid and elastic layers is allowed, but in the current version only a fluid sedimentary layer over elastic half space is implemented. The thickness of the sediment and the material properties are allowed to vary with range.

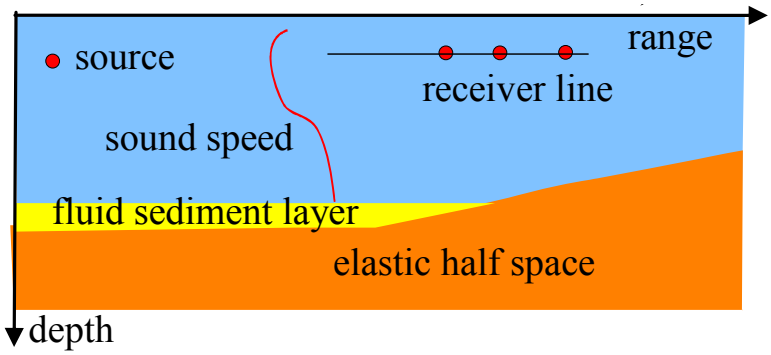

Figure 1. The model computes the received field from a source to receivers located on a horizontal line. The sound speed profile is only function of depth but the bathymetry and the layering in the bottom are allowed to vary with range.

The input information to the model is the range-dependent bathymetry, a sound speed profile (SSP) and the source location and the receiver depth. The initial ray tracing is done by launching a number of rays (typically 100 rays), with angles selected to cover the entire space between the source location and out to receivers on a horizontal line at the specified receiver depth.

The theory of ray is well known and shall not be developed here [Officer (1958), Clay and Medwin (1977), Jensen et al. (1993), Hovem (2010)]. The implementation used in the PlaneRay model is to divide the water column into a large number of layers with the same thickness Δz.

This layer thickness is also used as the depth increment in the calculations and generally the accuracy of the modelling improves with a finer depth increment. Typically the layer thickness is chosen to be about 1%, or less, of the water depth.

Within each layer, the sound speed is approximated with a straight line so that, in the layer $z_i<z<z_{i+1}$, the sound speed can be written

$$c(z) = c_i + (z - z_i)\, g_i \,, \tag{1}$$

where c_i is the sound speed at depth z_i, and g_i is the sound speed gradient in the segment approximated by

$$g_i = \frac{c(z_{i+1}) - c(z_i)}{(z_{i+1} - z_i)}. \tag{2}$$

Since the sound speed in each of these layers has a constant gradient, the ray in each layer follows a circular arc; the arc's radius of curvature $P_i(z)$ is given by the local sound speed gradient $g_i(z)$ and the ray parameter ξ,

$$P_i(z) = -\frac{1}{\xi g_i(z)}. \tag{3}$$

The ray parameter is defined as:

$$\xi = \frac{\cos(\theta_s)}{c(z_s)}, \tag{4}$$

where θ_s is the initial angle of the ray's trajectory at the source depth z_s and the sound speed is $c(z_s)$. After travelling through the layer from z_i to z_{i+1} the range increment is

$$r_{i+1} - r_i = -P_i(\sin\theta_{i+1} - \sin\theta_i), \tag{5}$$

which also can be written in the form

$$r_{i+1} - r_i = \frac{1}{\xi g_i}\left[\sqrt{1-\xi^2 c^2(z_{i+1})} - \sqrt{1-\xi^2 c^2(z_i)}\right], \tag{6}$$

and the travel time increment is

$$\tau_{i+1} - \tau_i = \frac{1}{|g_i|}\ln\left(\frac{c(z_{i+1})}{c(z_i)}\frac{1+\sqrt{1-\xi^2 c^2(z_i)}}{1+\sqrt{1-\xi^2 c^2(z_{i+1})}}\right). \tag{7}$$

The calculation of the trajectories and travel times described above assumes that the ray's curvature is finite, i.e. that the sound speed gradient is non-zero. In real life this will always be the case. However, in testing and in some other studies it is useful to have the possibility of using a constant sound speed; in such cases Equation (6) and Equation (7) is replaced with

$$r_{i+1} - r_i = \frac{|z_{i+1} - z_i|}{\tan\theta_{i+1}}. \tag{8}$$

$$\tau_{i+1} - \tau_i = \frac{|z_{i+1} - z_i|}{c_{i+1}\sin\theta_{i+1}}. \tag{9}$$

When the water depth varies with range, the ray parameter is no longer constant, but changes with the bottom inclination angle from θ_{in} to θ_{out} according to

$$\xi_{out} = \frac{\cos(\theta_{out})}{c} = \frac{\cos(\theta_{in} \pm 2\alpha)}{c} \quad , \tag{10}$$

depending on the sign of the ray angle and the angle of bottom slope.

The acoustic intensity is calculated by using the principle that the power within a space limited by a pair of rays with initial angular separation of $d\theta_0$ centered on the initial angle θ_0 will remain between the two rays, regardless of the rays' paths.

The acoustic intensity as function of horizontal range $I(r)$ is according to this principle given by

$$I(r) = I_0 \frac{r_0^2}{r} \frac{\cos\theta_0}{\sin\theta} \left| \frac{d\theta_0}{dr} \right| \quad . \tag{11}$$

Equation (11) predicts infinite intensity under two conditions, when θ=0 and when $dr/d\theta_0$=0. The first condition signifies a turning point where the ray path becomes horizontal; the second condition occurs at points where an infinitesimal increase in the initial angle of the ray produces no change in the horizontal range traversed by the ray. The locations where $dr/d\theta_0$=0 are called caustics, in the examples to follow exhibits many of these. The infinite intensity predicted by Equation (11) under these to condition is a limitation of ray theory. In reality and in both cases there is focusing of energy to a very high level, but the actual level is not predicted by classical ray theory.

2.1 Initial ray tracing

The equations above are applied to calculate the trajectories for a number of rays spanning the whole range of initial angles that are relevant for the actual studies. All receivers are assumed to be located at the same depth as specified by the user. For each ray, the intersection with the receiver depth is detected and the travel time, the ray angles at the receiver depth are calculated: This information is stored together with the ray history in terms of angles and coordinates of where the rays have been reflected from the bottom and surface, and where the rays have gone through turning points. Since the sound speed profile and the bathymetry are supposed to be fixed, and not changed, this ray tracing calculation is only done once for each scenario. Typical plot of SSP and ray trajectories are shown in Figure 1 showing rays from a source at 30 m depth with initial angles in the range of -30° to +30°.

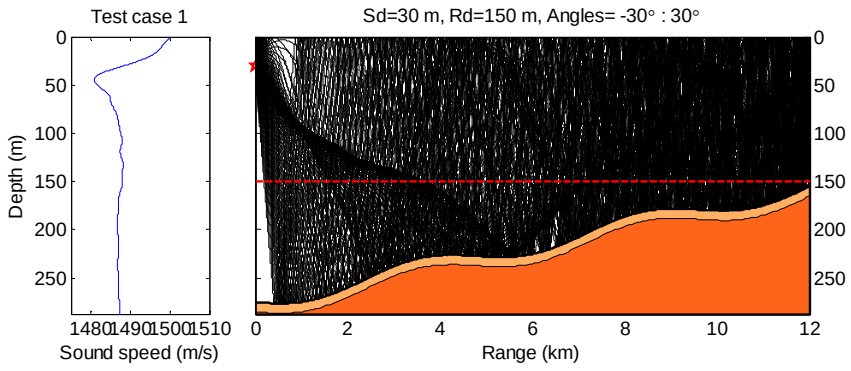

Figure 2. Sound speed profile and ray traces for a typical case. The source depth is 30m and the initial angles of the rays are between –30° to 30°.

2.2 Eigenray determinations

The next step is to determine the eigenrays and their trajectories. The approach used in PlaneRay is based on interpolation on the results and history of the initial ray tracing. To facilitate the interpolation, the rays first have to be sorted into groups or classes where the rays have the same type of history. The principle of sorting and interpolation is best illustrated with an example.

Figure 3 (left) shows result of the ray history of Figure 2, plotting the range to the receiver depth as function of the launch angle of the rays at the source. From this plot we see for instance at the range of 2 km there are 5 or 6 eigenrays; by reading from the plot we can determine approximately the values to be 10º, 2.5º,-2.5 º, two values at about -7 º and -11.5º. However, these values are not sufficient accurate for determination of the sound field and Equation (11) in particular. The displayed angle-range values are isolated points, but the display suggests the points can be grouped into curved continuous segments that are amendable to interpolation. The next step is to classify the points and rays into segments that have same path characteristics and that are single valued. Using the recorded ray history we classify the rays by the sign of the start angle of ray, and by the numbers of reflections at the bottom and sea surface and how many upper and lower turning points the ray has experienced.

The procedure with sorting and interpolation is explained in more detail in the article by Bao, Hovem and Yan (2010) and will not be discussed further here. However, a final result is the determination of initial angles and trajectories of all eigenrays between the source and receivers at any range at the specified receiver depth, together with the travel times, the locations and angles at the surface and bottom. Furthermore, the geometrical transmission loss is obtained by numerical evaluation of Equation (11). The right part of Figure 3 shows the geometrical transmission loss for each of the ray classes separately, but bottom losses and absorption losses are not included. The total transmission loss is obtained by coherent addition of all the contributions and includes bottom and surface reflection losses and absorption. The transmission loss is computed and discussed in section 3.3.

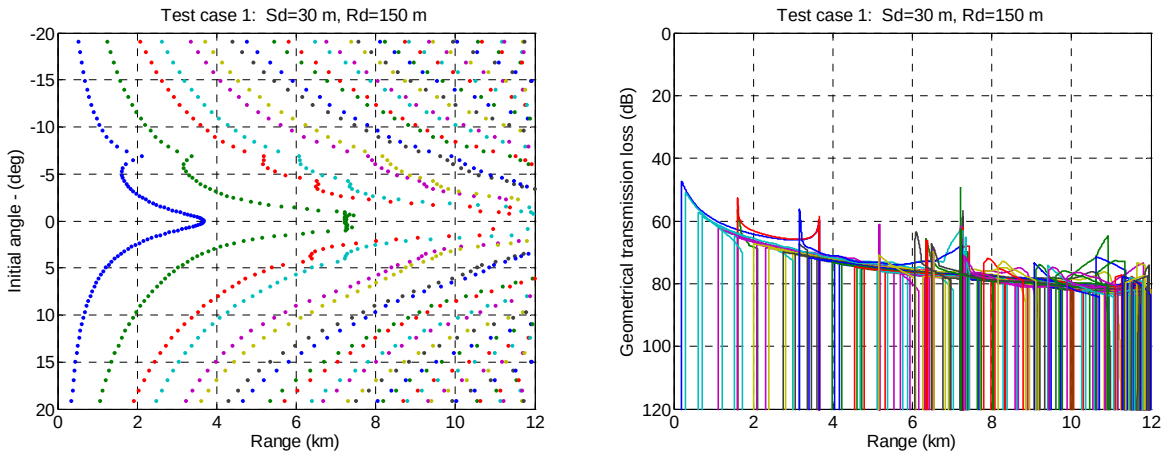

Figure 3. Left:Range to the given receiver depth as a function of initial angle at the source. Right: Geometrical transmission loss as function of range for the various ray types

The effects of caustics and turning points are clearly visible in Figure 3 as the exceptional low transmission losses at certain ranges such as at 1.8 km, 3.8 km, 5 km, and 7 km. As stated before, ray theory only predicts the location in space of the points, not the correct level.

Figure 4 shows as an example a plot of eigenrays from the source to a receiver at 150 m depth at a distance of 3 and 5 km. When using the PlaneRay model it is a good practice to check that the eigenrays are correct before proceeding with the analysis. The accuracy of the eigenray calculations is normally improved by using a higher density of rays in the initial ray tracing and by using a finer depth resolution.

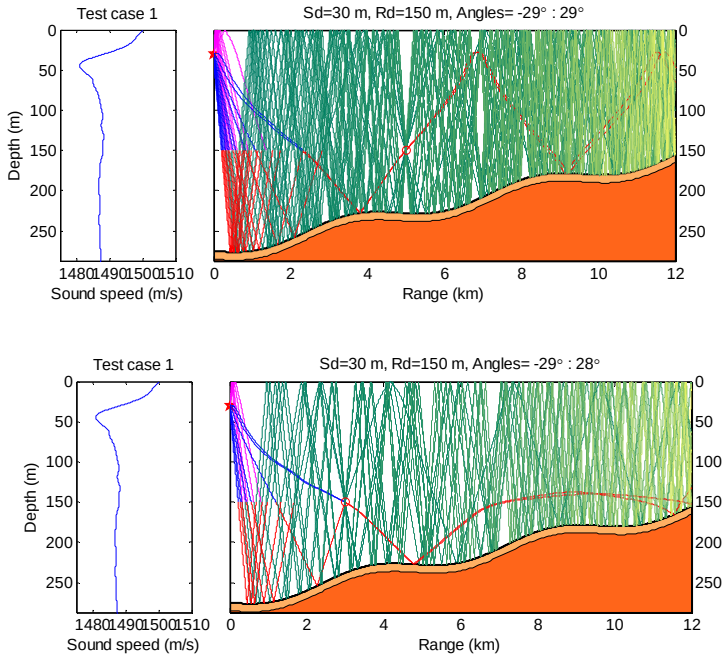

Figure 4. Eigenrays to a receiver at 150 m depth and distance of 3 km and 5 km from source.

2.3 Synthesizing the complete wave field by coherent addition of eigenrays contributions

The total wave field at any point along the receiver line is calculated in the frequency domain by coherent summation of all the eigenray contributions. This gives the complex frequency transfer function of the responses.

The transmission loss (TL) is given as the normalized absolute value of the frequency transfer function. Figure 5 shows an example where the transmission loss curves for the frequencies of 25 Hz, 50 Hz, 100 Hz, and 200 Hz are plotted as function of range. The dashed black line indicates spherical spreading loss. Note the very high level, low transmission loss, at little more than 7 km. This is due to the caustic we have mentioned earlier.

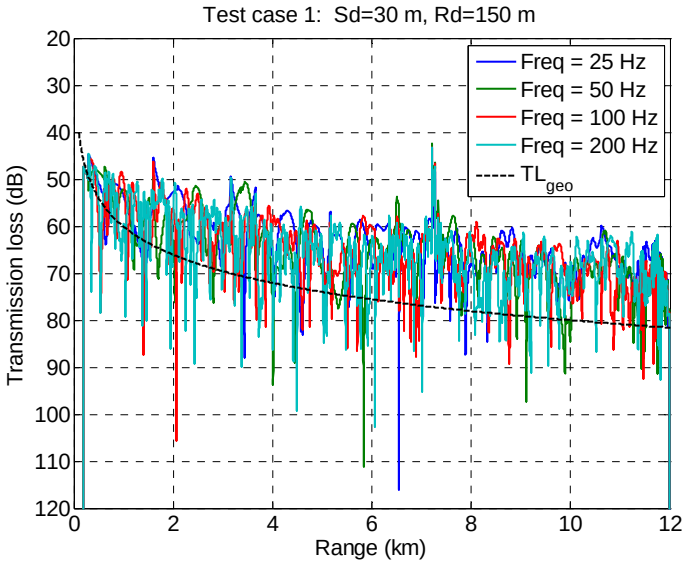

Figure 5. Transmission loss as function of range calculated for the frequencies of 25 Hz, 50 Hz, 100 Hz, and 200 Hz. The dashed black line indicates spherical spreading loss.

The time domain solution is obtained after multiplication with the frequency function of a source signal and by an inverse Fourier transform of the product. This requires that the user defines a source signal, a sampling frequency (f_s) and a block length (*nfft*) of the Fourier transform. In the basic PlaneRay model only a simple Ricker pulse is implemented as a source pulse.

Figure 6 shows an example of which Ricker pulse and its frequency spectrum. In this case the centre frequency of the pulse is 100 Hz, but this parameter can be chosen by the user. A good sampling frequency of such a pulse is about 10 times the centre frequency. The total duration of the time window ($T_{\max}$) after Fourier transform is

$$T_{\max} = nfft / f_s \,. \tag{12}$$

It is very important that *nfft* and f_s are selected so that Fourier time window, $T_{\max}$, is larger than the actual length of the signal.

Figure 8 shows a number of time responses as function of range and time. The time scale is here in real time, i.e. the total time between the Ricker pulse has been emitted from the source to response is received at the receiver. Notice again the high values caused by the caustics at3 km, 6, km and 7 km. A more convenient plot is shown in Figure 8 where the same time response are plotted as function of reduced time, defined as

$$t_{red} = t_{real} - \frac{r}{c_{red}} \,. \tag{13}$$

In Equation (13) t_{real} and t_{red} are the real and reduced times respectively, r is range and c_{red} is the reduction speed. The actual value of c_{red} is not important as long as the chosen value results in a good display of the time responses.

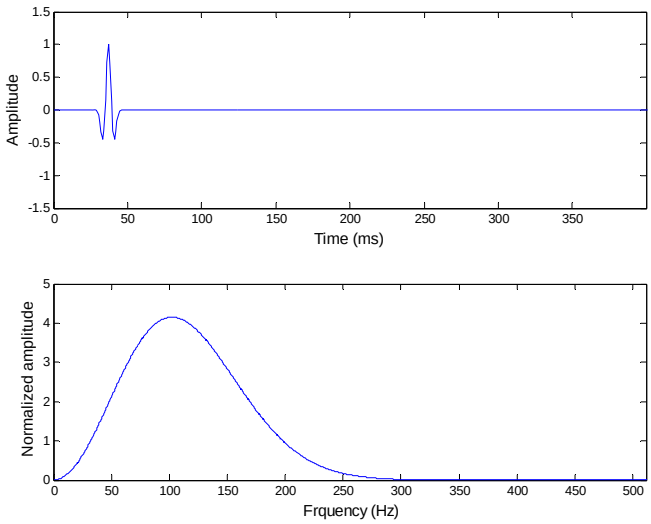

Figure 6. The Ricker pulse source signal used in the examples of this report with the time signal in the upper apart and its frequency spectrum in the lower part.

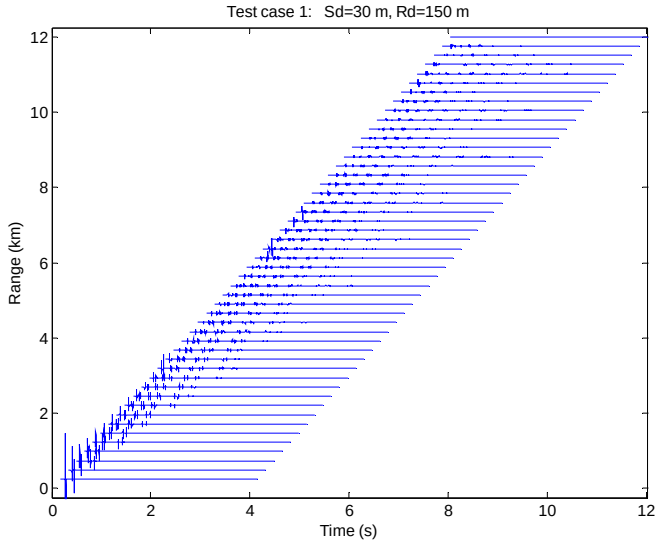

Figure 7. Received time responses as function of range and plotted as functions of real time.

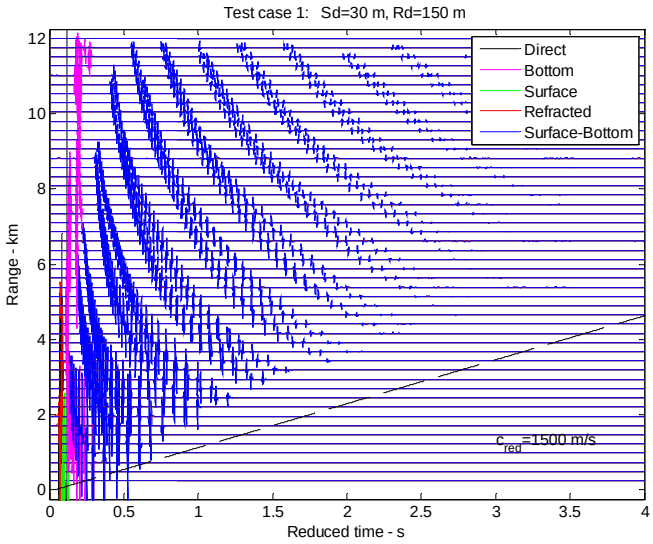

Figure 8. Received time responses as function of range and plotted as functions of reduced time.

3 Comparison with the OASES model

As stated before, we intend to supplement PlaneRay calculation with results from using the propagation model OASES, primarily in situations where ray theory may be inaccurate. The OASES (or SAFARI) model is an acoustic propagation model based on the wave number integration technique developed by Schmidt (1987, 1993). The basic model, this is the only model available to us, can only treat range independent environments and thus not situations with varying bathymetry. As a preliminary exercise this section shows a number of examples with comparison between the PlaneRay and OASES, the examples are intended to illustrate the fundamental limitations of the ray trace models.

The first examples considers the so called Pekeris case [Pekeris (1948)] where the water has constant depth and sounds speed, the bottom is homogenous an treated as a fluid and sound speed c_{p1} density ρ_1, and absorption $\alpha_{p1.}$ We show examples with water depth of 100 m and with 300 m and with different source and receiver depths.

Figure 9 shows the case where the water depth is 100 m, the source is at 25 m depth and the receivers are located on a line at 75 m depth out to a range of 30 km. The figure compares the transmission loss at 50 Hz and 100 Hz obtained by using OASES (red) and PlaneRay (blue).

The two sets of results are very close except for the lowest frequency of 25 Hz, where there is a minor shift in the interference pattern.

In Figure 10 the water depth is increased to 300 m and the depth of the source is the same (25 m) but the receiver depth is now 275 m, which is at the same height above the bottom as in the previous case. Now the PlaneRay and the OASES results agree quite well also for the 25 Hz.

These results confirm the commonly accepted rule which says that ray theory is adaptable down to frequencies where the water depth is more than two times of the acoustic wave length

This gives a rough measure of the minimum frequency f_{min} for the validity of ray theory for a given water depth d and sound speed c.

$$f_{\min} = 2\frac{c}{d}. \tag{14}$$

In our case the water depth of d=100 m gives f_{min}=100 Hz, and d=300 m gives f_{min}=10 Hz. For lower frequencies we will supplement the PlaneRay calculations with OASES results when applicable.

The next examples compare PlaneRay and OASES in situations where the seabed is layered with a sediment layer over hard bedrock.

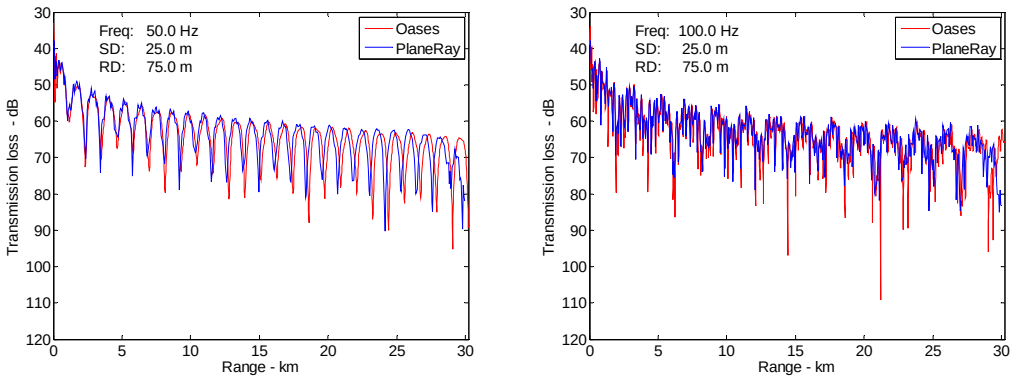

Figure 9. Transmission loss as function of range for a frequency of 50 Hz and 100 Hz. Comparison of the PlaneRay and the OASES results. Pekeris wave guide with water depth 100 m over a sandy bottom with sound speed c_{p1}=1700m/s, ρ_1=1800kg/m^3, α_{p1}=0.1 dB/wavelength.

Figure 11 shows a case similar to that shown in Figure 10 except that the bottom has a fluid sediment layer with thickness 10 meter fluid layer over a solid half space. The sound speed in the sediment layer is 1700 m/s, and the density is 1800 kg/m^3. The solid half space has compressional speed of 3500 m/s, shear speed 1000 m/s, and density 2500 kg/m^3.

Figure 12 shows the situation where the receiver (the fish) is located one meter above the bottom, which has a 20 m thick sediment layer over hard bedrock. The general agreement of the results are quite good and judge to be acceptable for the study of fish reactions to seismic noise .

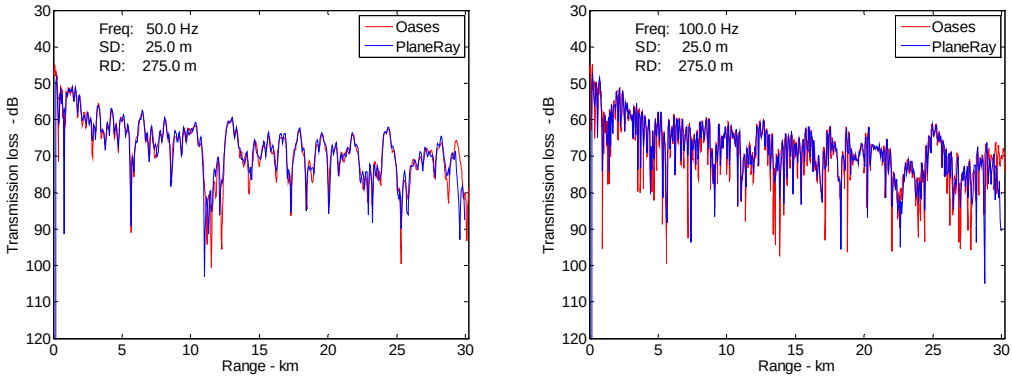

Figure 10. Transmission loss as function of range for a frequency of .50 and 100 Hz. Comparison of the PlaneRay and the OASES results. Pekeris wave guide with water depth 300 m over a sandy bottom with sound speed c_{p1}=1700m/s, ρ_1=1800kg/m^3, α_{p1}=0.1 dB/wavelength.

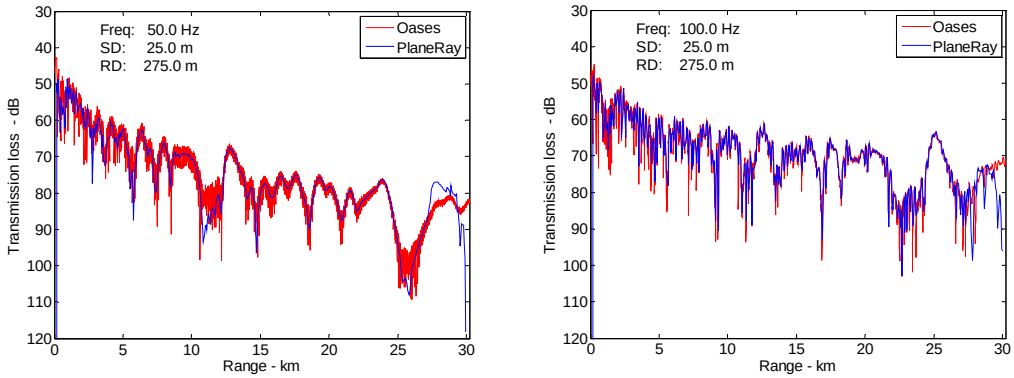

Figure 11. Transmission loss as function of range for a frequency of 50 Hz and 100 Hz. Comparison of the PlaneRay and the OASES results. Water depth 300 m, layered bottom with a 10 meter fluid layer over a solid half space. Fluid layer: sound speed 1700 m/s, density 1800 kg/m^3, solid half space: compressional speed 3500 m/s, shear speed 1000 m/s, density 2500 kg/m^3

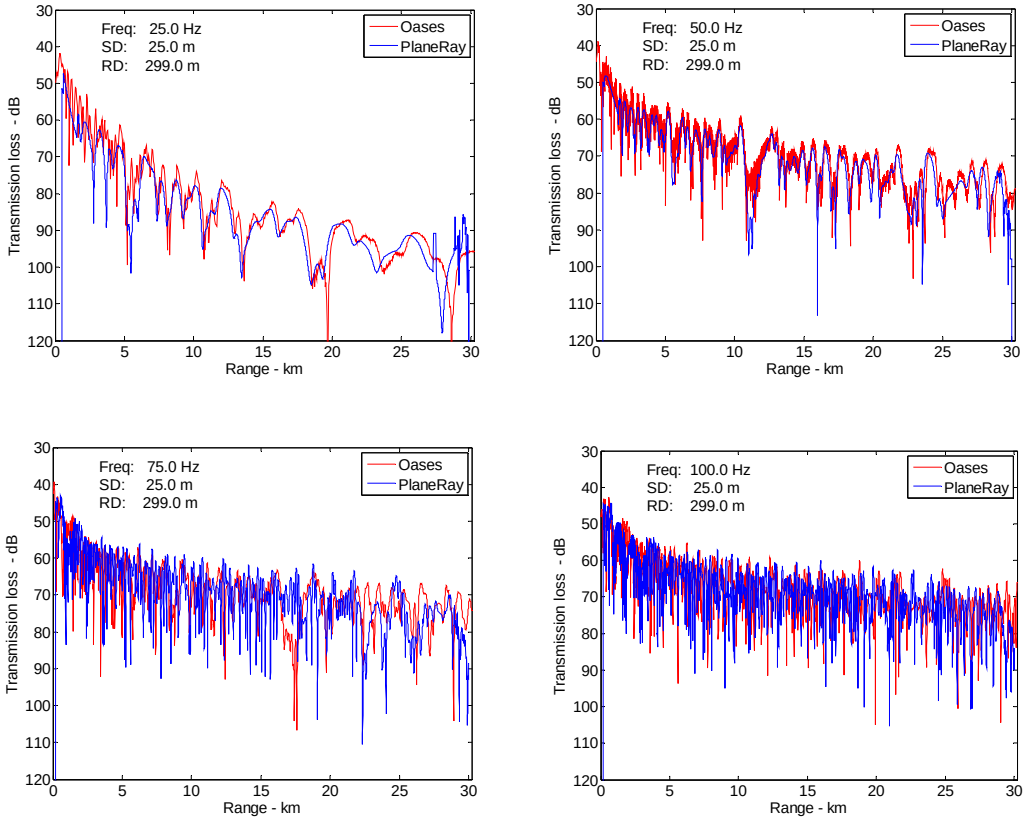

Figure 12. Transmission loss as function of range for a frequency of 20 Hz to 200Hz. Comparison of the PlaneRay and the OASES results. Water depth 300 m, layered bottom with a 20 meter fluid layer over a solid half space. Fluid layer: sound speed 1700 m/s, density 1500 kg/m^3, solid half space: compressional speed 3500 m/s, shear speed 1000 m/s, density 2500 kg/m^3. All absorptions are 0.1 dB/wavelength.

4 Post-modelling programs

In addition to the propagation models describe so far, there will be number of application programs intended for post modelling applications. These programs are designed to input both the modelling results and the real life data obtained by experiments at sea the. Typically the input data will be recorded and modelled time signals. The development of these programs will be in close collaboration with the marine biologist and the programs adapted to test various criteria for fish perceptions and reactions to air gun generated acoustic signals. As an example, the next section will address how fast the acoustic field is decaying away with increasing distance from the source.

4.1 Transmission loss and sound pressure level as function of range.

The issue of how fast the acoustic field is decaying is frequently debated. Some claims that the field decays as spherical spreading other prefers cylindrical spreading, which gives a geometrical transmission loss of $-20\log(r/r_0)$ or $-10\log(r/r_0)$, respectively. Here, r_0 is a reference distance normally 1 meter.

We discuss this issue by using a simple case of a Pekeris wave guide with a flat bottom at 100 m depth and with sound speed c_{p1}=1700m/s, density ρ_1=1500kg/m^3, and absorption α_{p1}=0.1 dB/wavelength. Figure 13 shows the time series of the signals received at various distances and Figure 14 show the transmission loss as function of range for some selected frequencies. The transmission losses have been calculated by integration over full duration of the signals in Figure 13. As can be seen, the transmission losses are bracketed between spherical and cylindrical transmission losses.

Alternatively to the transmission loss displayed in Figure 14 it might be more relevant to evaluate how the peak sound pressure decays with distance from the source. This is shown in Figure 15 (left). As can bee the peak sound pressure values decay at a rate close to spherical propagation i.e. as 20 log(r).

Another interesting parameter is the root mean square (rms) pressure of the received signals calculated as

$$p_{rms} = \sqrt{\frac{1}{N}\sum_{n=0}^{N-1}(p_n)^2}\,, \tag{15}$$

where p_n are the sound pressure samples and N is the total nominal length of time window measured in sample numbers. Notice that N is the same sample number for traces regardless of the range. The total signal energy is therefore proportional to

$$E = N(p_{rms})^2 = \sum_{n=0}^{N-1}(p_n)^2\,. \tag{16}$$

In Figure 15 (right) the rms pressure, normalized with respect to the rms pressure of the source signal and converted to dB, is displayed as function of range. The rms pressure is decaying at rate close to cylindrical spreading 10 log(r).

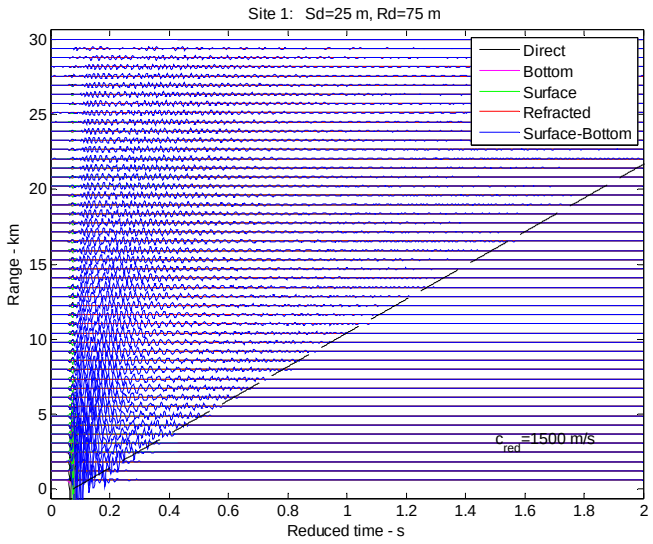

Figure 13. Pulse responses as function of time and range for a Pekeris wave guide with water depth 100 m over a sandy bottom with parameters c_{p1}=1700m/s, ρ_1=1500kg/m^3, α_{p1}=0.1 dB/wavelength. The black dashed line indicates the critical angle time duration limit.

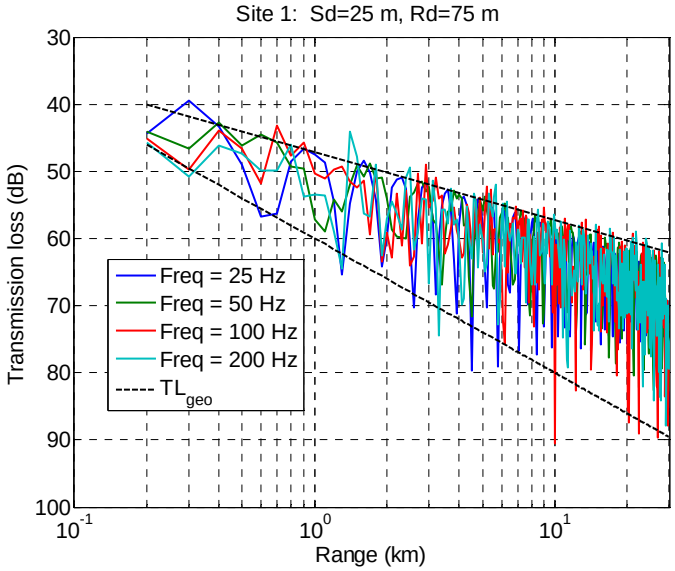

Figure 14. Transmission loss as function of range for the selected frequencies of 25, 50, 100, and 200 Hz for a Pekeris wave guide with water depth 100 m over a sandy bottom with parameters c_{p1}=1700m/s, ρ_1=1500 kg/m^3, α_{p1}=0.1 dB/wavelength. The black dashed lines are the decay rates for geometrical and cylindrical spreading.

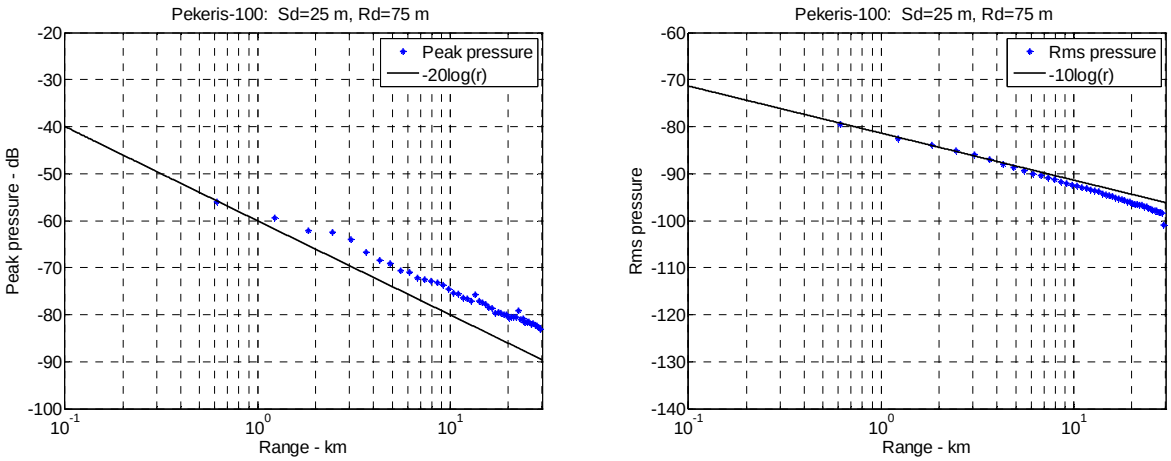

Figure 15. Peak pressure (left) and rms pressure (right) as function of range. Pekeris wave guide with water depth 100 m over a sedimentary bottom with c_{p1}=1700m/s, ρ_1=1500kg/m^3, and α_{p1}=0.1 dB/wavelength. The black line is transmission losses for geometrical spherical and cylindrical spreading, respectively.

The same processing is applied to the test case defined by Figure 2 and the time signal shown in Figure 8. This is a more realistic case, but the results are similar to the results of the previous ideal case. The rms pressure decays generally according to cylindrical spreading and the peak pressure according to spherical spreading but the peak values in certain locations may attain significantly higher values. These high values are caused by the focussing and concentrations in the caustics as earlier discussed.

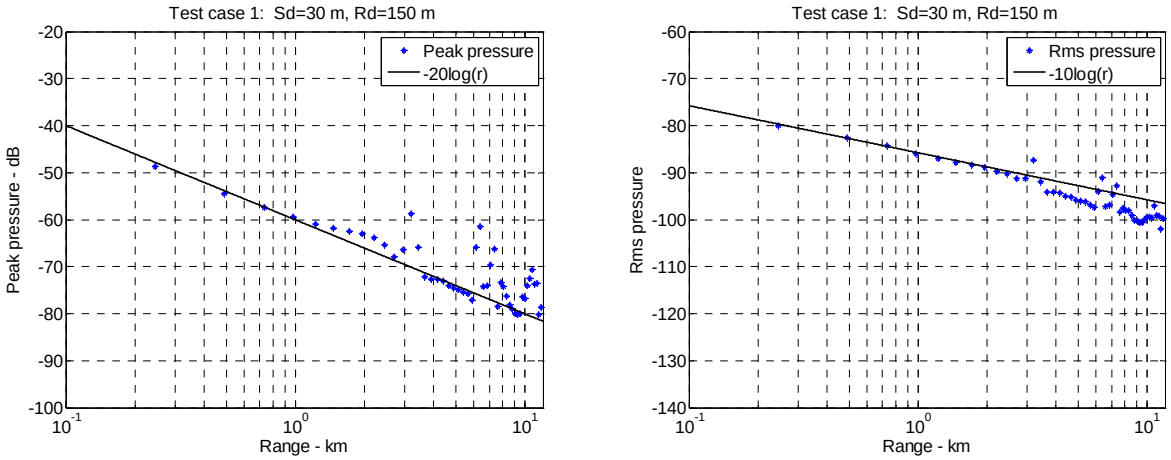

Figure 16.Peak pressure (left) and rms pressure (right) as function of range. based on the Test case 1 and the time signals displayed in Figure 8

References

Bao, Xueshan, Jens M. Hovem and Shefeng Yan, ”A novel method to determine eigenrays for acoustic propagation models based on ray theory”. Manuscript in preparation, December 2009.

Clay C. S. and H. Medwin, *Acoustical Oceanography: Principles and Applications*, Wiley-Interscience, USA, (1977).

Collins M. D., A split-step Pade solution for parabolic equation method, J. Acoust. Soc. Am. **93**, 1726-1742 (1993).

Collins M. D., User guide for RAM version 1.0 and 1.0p, (ftp:// ram.nrl.navy.mil/pub/ RAM/), (2001).

Hovem J. M., Marine Acoustics: *The Physics of Sound in Underwater Environments*, (To be published by Peninsula Publishing, Los Altos, CA, and Applied Research Laboratories, The University of Texas at Austin, Texas), 2010.

Hovem Jens M." PlaneRay: An acoustic underwater propagation model based on ray tracing and plane wave reflection coefficients" in *Theoretical and Computational Acoustics* 2007, Edited by Michael Taroudakis and Panagiotis Papadakis, Published by the University of Crete, Greece, 2008. pp. 273-289 (ISBN: 978-960-897854-2).

Hovem, J. M. "PlaneRay: An Acoustic propagation model based on ray tracing and plane-ray reflection coefficients" Norwegian Defense Research Establishment (FFI) Report no 08/00610, March 2008.

Jensen F. B. and M. C. Ferla, “SNAP: The SACLANTEN normal-mode acoustic propagation model,” SM-121, SACLANT Undersea Research Centre, La Spezia, Italy (1979).

Jensen F. B., W. A. Kuperman, M. B. Porter, and H. Schmidt, *Computational Acoustics*, AIP Press, New York Jersey, (1993).

Officer, C. B. *Introduction to the theory of sound transmission*. McGraw-Hill, New York City, 1958.

Pekeris A. L., The theory of propagation of explosive sound in shallow water, Geol. Soc. Am. Mem. **27** (1948).

Schmidt H., OASES 1.6: Application and upgrade notes, Massachusetts Institute of Technology, Cambridge, MA (1993).

Schmidt H., SAFARI: Seismo-acoustic fast field algorithm for range independent environments. User’s guide, SR-113, SACLANT Undersea Research Centre, La Spezia, Italy (1987).

Tindle C. T. and G. E. J. Bold, Improved ray calculations in shallow water, J. Acoust. Soc. Am. **70**(3), 813-819 (1981).

Westwood, E. K and C. T. Tindle, Shallow water time simulation using ray theory, J. Acoust. Soc. Am. **81**, 1752 -1761 (1987).

Westwood, E. K and P. J. Vidmar, Eigenray finding and time series simulation in a layered-bottom ocean, J. Acoust. Soc. Am. **81**, 912 -924 (1987).

Appendix Short user guide to PlaneRay.

The plane Ray model is run be activating the following statements:

```
%**********************Stage 1*****************************************
```

planeray

```
% This calls on the all the relevant PlaneRay programs and functions
% (1) Calls on the input programs to set up the input parameter and the
% environment file using the function planerayinput (the file para and env.
% % Set up the parameters files env. and para. _struct files containg all
%environmental parameters and parameters for the calculations.
Example=input( 'Example ? ')
rawinput = planerayinput(Example);
[env, para] = initpara(rawinput);
%**********************Stage 2*****************************************
[EIG, COUNT, SUFBOT, Rays] = tracerays(env, para);
% Perform the initial ray tracing and produce figure(1) with ray traces
% and sound speed profile. %If not what you want, stop at this point and go
back to Stage 1.
%**********************Stage 3*****************************************
[eigenangle, EIG, COUNT, SUFBOT, Rays, para]=plotrays(EIG, COUNT, SUFBOT,
Rays, env, para);
%
% Main program for sorting and interpolation of the ray history and
% produces the EIG results. The result can be displayed and by calling  the
optional program in Stage 4:
 %**********************Stage 4*****************************************
 ploteigstructure(Rays, EIG, COUNT, env, para);
% Produces plots of range to receiver array as function of initial angle,
% and geometrical spreading loss as function of range for each ray class
% Make sure that you understand the results before continuing.

%**********************Stage 4************************
ang=ploteigenray(eigenangle,env,para,EIG.count)
%  Optional
%  Calculate the trajectories of the eigenrays to receivers at spcified range;
%  This program must be executed after running plotrays.m

%*********************************5 *********************************
TL=plottransloss(EIG, COUNT, SUFBOT, env, para );
% Produces plots tramsmission loss for the frequency specified in
% in para.frequency
% This result is obtained by coherent addition of all eigenray contributions
% and includes the standard seawater absorption for the actual frequency
% Plots are numbered from 10 to 12

%*********************************6 *********************************
 source_signal, fs,t_0] = getsourcesignal(1,para);
[signal, h, eigen]=plotresponse(EIG, COUNT, SUFBOT, env, para, source_signal,
fs,t_0);
%Procdues the time responses as received at ranges specified in
para.range_phone
%The source pulse is generated in the getsourcesignal(source_type,para)
% source_type=1, is a Ricker pulse, other types must be implemented by the
user.
%*************************************************************
```

Input files

The input values are activated by the program planerayinput.

```
function rawinput = planerayinput(Example)
PLR_initial_settings; %This program set the parameters most likely to be used but can be
overruled by statements below;
 switch Example;
      case 0
      title_tekst='Test case 1'; %Give a title to the case you are running

      %******************SOUND SPEED PROFILE**********************
      % Specify the sound speed profile any way you want, but end up with
      % assigned values for c_input and z_input
      % Example where the raw data is contained in a file with name ssp_case_0;
 load ssp_case_0;ssp=ssp_case_0;
c_input=ssp(:,2); z_input=ssp(:,1);
      %The sound speed profile will later be interpolated to of equal depth spacing of del_z;
del_z=0.5;
if c_input(1)~=c_input;islinear=1;else islinear=1; end%
      % Special ray tracing algorithm for constant sound speed

      %*********************GEOMETRY************************************
R_max=10000;    % Maximum range in meter for ray calculations
N=50000;        % Max number of calculated points per ray
z_source=7.5;    % Source depth in meter Pekeris
z_receiver=250;  % Receiver depths in meter
range_source=0; % Range position of the source.

      %*********************BOTTOM TOPOGRAPHY**************************
      %Bottom topography is described with the range R_b where the depth is Z_b;
      % The user has to write, or generate, the range-depth coordinates.
      % This is an example of a gently upward rolling hill:
R_b=[0:1: R_max];   z_max=max(z_input);
Z_b=z_max-R_b*0.01+ 10*sin(pi*(5*R_b/R_max));

      %***************PHYSICAL PARAMETERS OF BOTTOM**************

cp1=1700; ap1=0.1; rho1=1500;
cp2=3500; ap2=0.1; rho2=3500;
cs2=1000;as2=0.1;lay_thick=20;

      %***************PARAMETERS FOR THE RAY TRACING*************

        % Spcifiations of the angles for the initial ray tracing. This example yields a higher
        % densities of angles close to horizontal direction. Often a good practice.
 N_angle=30;   theta_max=30; n=1:N_angle;
ang=theta_max.^(n/N_angle)-theta_max.^(1/N_angle) ;ang=ang(ang>0);
start_theta=sort([-ang ang]);
```

searcheigenray=0;
% If problem with eigenray accuracy set this parameter =1, otherwise 0;
bottom_stop=0;
%The ray tracing will stop after "bottom_stop>0" number of reflections
surface_stop=0;%The ray tracing will stop after "surface_stop>0" number of surface reflections.

%*********DISPLAY and SIGNAL PROCESSINGPARAMETERS**********

fs=1024; Sampling frequency for the calculation of the transfer function and the time responses
nfft=2048; %Block length for the Fourier transformation to time domain.
% Time window length is T_max=nfft/fs.
%Watch out for aliasing errors in the time responses
frequency=[25 50 100 200];% Frequencies for calculation of transmission loss.
range_receiver=linspace(0,R_max,51);
range_TL=range_receiver;

%**********END**********